Conservation laws and multiplicity evolution of spectra at energies available at the BNL Relativistic Heavy Ion Collider

Zbigniew Chajęcki* and Mike Lisa†
Department of Physics, Ohio State University, 191 West Woodruff Ave., Columbus, Ohio 43210, USA
(Received 24 July 2008; published 23 March 2009; publisher error corrected 29 June 2009)

Transverse momentum distributions in ultrarelativistic heavy ion collisions carry considerable information about the dynamics of the hot system produced. Direct comparison with the same spectra from $p + p$ collisions has proved invaluable in identifying novel features associated with the larger system, in particular, the "jet quenching" at high momentum and the apparently much stronger collective flow dominating the spectral shape at low momentum. We point out possible hazards of ignoring conservation laws in the comparison of high- and low-multiplicity final states. We argue that the effects of energy and momentum conservation actually dominate many of the observed systematics, and that $p + p$ collisions may be much more similar to heavy ion collisions than generally thought.

DOI: 10.1103/PhysRevC.79.034908 PACS number(s): 25.75.Gz, 25.70.Pq

I. INTRODUCTION

A. Heavy ion physics: Relying on comparison

The physics program at the Relativistic Heavy Ion Collider (RHIC) at Brookhaven National Laboratory is remarkably rich, thanks to the machine's unique ability to collide nuclei from ^{1}H to ^{197}Au, in fully symmetric (e.g., Au + Au or $p + p$) to strongly asymmetric (e.g., d + Au) entrance channels, over an energy range spanning more than an order of magnitude. The capability to collide polarized protons provides access to an entirely new set of fundamental physics, not discussed further here.

Achieving the primary aim of RHIC—the creation and characterization of a color-deconfined state of matter and its transition back to the confined (hadronic) state—requires the full capabilities of RHIC. In particular, comparisons of particle distributions at high transverse momentum (p_T) from Au + Au and $p + p$ collisions probe the color-opaque nature of the hot system formed in the collisions [1–3]. Comparisons with reference $d + A$ collisions were necessary to identify the role of initial-state effects in the spectra [4]. Comparing anisotropic collective motion from noncentral collisions of different-mass initial states (e.g., Au + Au vs Cu + Cu) [5] tests the validity of transport calculations crucial to claims of the creation of a "perfect liquid" at RHIC [6]. Indeed, a main component of the future heavy ion program at RHIC involves a detailed energy scan, designed to identify a predicted critical point in the equation of state of QCD [7].

The need for such systematic comparisons is not unique to RHIC, but has been a generic feature of all heavy ion programs [8,9], from low-energy facilities such as the National Superconducting Cyclotron Laboratory (NSCL) at Michigan State University to progressively higher energy facilities such as the GSI heavy ion synchrotron (SIS), Bevatron/Bevalac at Berkeley Lab, BNL Alternating Gradient Synchrotron (AGS), and CERN Super Proton Synchrotron (SPS). The nature of heavy ion physics is such that little is learned through the study of a single system.

B. Bigger is better

Despite the necessary attention given to smaller colliding partners, these comparisons are ultimately aimed at identifying novel aspects of collisions between the heaviest ions, in which a highly excited *bulk system* might be created, with a sufficient number of degrees of freedom such that it may be described thermodynamically, e.g., in terms of pressure, temperature, energy density, and an equation of state (EOS). If the energy density of this system is sufficiently large (typically estimated at $\epsilon_{\rm crit} \sim 1$ GeV/fm^3 [6]) and its spatial extent considerably larger than the color-confinement length $\sim$1 fm, then a new state of matter—the quark-gluon plasma (QGP) [10]—may be created. Microscopically, such a state might be characterized by colored objects (or something more complicated [11]); macroscopically, it represents a region on the phase diagram in which the EOS is distinctly different from that for the hadronic phase [12].

Ultrarelativistic collisions between the heaviest nuclei enjoy the additional advantage that finite-size effects are small, due to high-multiplicity final states. In a small system (e.g., final state of a $p + \bar{p}$ collision), a statistical analysis of yields requires a canonical treatment because of the conservation of discreet quantum numbers such as baryon number and strangeness [13]. For larger systems, a grand canonical treatment is more common, e.g., Ref. [14], with finite quantum-number effects absorbed into, e.g., "saturation factors" [15].

Because of the large available energy $\sqrt{s}$ and final-state multiplicity, energy and momentum conservation effects on kinematic observables (spectra, momentum correlations, elliptic flow) are generally small. They are accounted for with correction factors [16,17] or neglected altogether.

C. Multiplicity evolution of single-particle spectra

Detailed single-particle spectra (e.g., d^2N/dp_T^2) have been measured at RHIC for a variety of particle types. Often, the

*chajecki@mps.ohio-state.edu
†lisa@mps.ohio-state.edu

shape of the "soft" ($p_T \lesssim 2$ GeV/c) part of the spectrum is compared with hydrodynamic calculations [18] or fitted to simple "blast-wave" parametrizations, e.g., Ref. [19], to extract the collective flow of the system. The "hard" sector ($p_T \gtrsim 4$ GeV/c) is assumed to be dominated by the physics of the initial-state, high-Q^2 parton collisions and resulting jets. The physics of the "firm" sector ($2 \lesssim p_T \lesssim 4$ GeV/c) may be the richest of all, reflecting the dynamics of the confinement process itself [20].

We would like to focus not so much on the single-particle spectra themselves but on their multiplicity dependence. Much has been inferred from this dependence. In the soft sector, blast-wave fits to spectra from high-multiplicity final states (associated with central $A + A$ collisions) indicate strong collective radial flow; the same fits to low-multiplicity final states—including minimum-bias $p + p$ collisions—appear to indicate much weaker flow [21]. This seems to confirm a common assumption that $p + p$ collisions are not sufficiently "large" to develop bulk collective behavior.

In the hard sector, one of the earliest and most exciting observations [3,22] at RHIC was that the high-p_T yield from high-multiplicity Au + Au collisions was suppressed, relative to appropriately scaled lower multiplicity $A + A$ or minimum-bias $p + p$ collisions. This has been taken as evidence of energy loss of hard-scattered partons through a very color-dense medium. Meanwhile, the high-p_T part of the spectrum from high-multiplicity $p + p$ collisions appears *enhanced* relative to low-multiplicity $p + p$ collisions [23], again suggesting that a color-dense bulk system is not produced in $p + p$ collisions.

In this paper, we discuss the effects of energy and momentum conservation on the multiplicity evolution of single-particle spectra at RHIC. Energy and momentum conservation-induced constraints (EMCICs)[1] have been largely ignored in the analyses just mentioned, probably for two reasons. The first is the field's usual focus on the highest multiplicity collisions, where such effects are assumed small; it seems natural to compare analyses of such systems to "identical" ones of smaller systems, forgetting that EMCIC effects play an ever-increasing role in the latter case. Perhaps the more important reason is that EMCICs do not generate "red flag" structures on single-particle spectra; this is in contrast to multiparticle correlation analyses, in which conservation-law-induced correlations may be manifestly obvious and have even been used to estimate the number of unmeasured neutral particles in high energy collisions [24]. Especially with the enhanced attention on precision and detail at the SPS and RHIC, there has been increasing discussion of EMCIC effects in two-particle [17,25], three-particle [26], and N-particle [27] observables. Below, we show that EMCIC effects on single-particle spectra are also significant and may even dominate their multiplicity evolution.

[1]In Ref. [25], we discussed energy and momentum conservation-induced *correlations* (EMCICs) in multiparticle distributions. In the present manuscript, we discuss these very effects with the same formalism, but projected onto the single-particle distributions. It is convenient and natural, then, to use the same acronym here, replacing "correlation" with "constraint."

D. Organization of this paper

Several authors (see, e.g., Ref. [28]) have discussed finite-number effects in statistical models, and many numerical simulations of subatomic collisions conserve energy and momentum automatically, e.g., Refs. [29,30]. However, as pointed out by Knoll [31], our question—to what extent do EMCICs *alone* explain the multiplicity evolution of spectra?—cannot be addressed from these simulations themselves, since in these models, the evolution of dynamics and kinematics are interwoven. Thus, in Sec. II, we discuss a formalism based on Hagedorn's generalization of Fermi's Golden Rule, in which dynamics and kinematics (phase space) factorize. This leads to a formula for finite-number effects on single-particle spectra, due solely to kinematics, for a fixed dynamical ("parent") distribution.

In Sec. III, we test the extreme ansatz that *all* of the experimentally measured multiplicity dependence of single-particle spectra is due to EMCICs. We will find surprising agreement with this ansatz in the soft sector ($p_T \lesssim 1$ GeV/c). We will discuss that our formalism is on less firm footing, conceptually and mathematically, at much higher p_T. Nevertheless, we explore this regime as well. We find that in the hard sector, the data from heavy ion collisions is clearly *not* dominated by EMCICs, though we point out that ignoring EMCICs, especially for $p + p$ collisions, may be dangerous even at high p_T.

In Secs. IV and V, we summarize and give an outlook for future studies.

II. EFFECTS OF ENERGY AND MOMENTUM CONSERVATION ON SINGLE-PARTICLE SPECTRA

A. Restricted phase-space factor

Changing the size (central vs peripheral ion collisions, $e + e$ collisions, etc.) and energy of a collision system will lead to different measured single-particle distributions, reflecting (1) possibly different physical processes driving the system and (2) effects due to phase-space restrictions. To focus on changes caused by the latter, we consider some Lorentz-invariant "parent" distribution $\tilde{f}(p) \equiv 2E\frac{d^3N}{dp^3}$, driven by some unspecified physical process, but *un*affected by energy and momentum conservation. For simplicity, we assume that all particles obey the same parent distribution.

In the absence of other correlations, the measured single-particle distribution is related to the parent according to [16,17,25,27]

$$\tilde{f}_c(p_1) = \tilde{f}(p_1)\frac{\int\left(\prod_{j=2}^{N} d^4p_j\,\delta\left(p_j^2 - m_j^2\right)\tilde{f}(p_j)\right)\delta^4\left(\sum_{i=1}^{N} p_i - P\right)}{\int\left(\prod_{j=1}^{N} d^4p_j\,\delta\left(p_j^2 - m_j^2\right)\tilde{f}(p_j)\right)\delta^4\left(\sum_{i=1}^{N} p_i - P\right)}, \tag{1}$$

where N is the event multiplicity. The integral in the numerator of Eq. (1) represents the number of configurations in which the $N - 1$ other particles counterbalance p_1 so as to conserve the total energy-momentum P of the event, and the denominator, integrating over all N particles, is a normalization.

For $N \gtrsim 10$ [25], one may use the central limit theorem to rewrite the factor in Eq. (1) as [16,17,25,27]

$$\tilde{f}_c(p_i) = \tilde{f}(p_i)\left(\frac{N}{N-1}\right)^2 \exp\left[-\frac{1}{2(N-1)}\left(\frac{p_{i,x}^2}{\langle p_x^2\rangle} + \frac{p_{i,y}^2}{\langle p_y^2\rangle} + \frac{p_{i,z}^2}{\langle p_z^2\rangle} + \frac{(E_i - \langle E\rangle)^2}{\langle E^2\rangle - \langle E\rangle^2}\right)\right], \tag{2}$$

where

$$\langle p_\mu^n\rangle \equiv \int dp\, \tilde{f}(p) p_\mu^n \tag{3}$$

are average quantities, and we have set the average three-momentum $\langle p_{(\mu=1,2,3)}\rangle = P_{\mu=1,2,3}/N = 0$. We stress that what appears in Eq. (3) is the parent distribution $\tilde{f}$, not the measured one $\tilde{f}_c$. Hence, for finite multiplicity N, the averages $\langle p_\mu^n\rangle$ are not the measured ones, which we define as

$$\langle p_\mu^n\rangle_c \equiv \int dp\, \tilde{f}_c(p) p_\mu^n. \tag{4}$$

See also the discussion in Appendix B.

Since p_T distributions are commonly reported, we would like to estimate EMCIC distortions to p_T distributions, integrated over azimuth and a finite rapidity bin centered at midrapidity. As discussed in Appendix A, for the approximately boost-invariant distributions at RHIC [21], the measured and parent p_T distributions are related by

$$\tilde{f}_c(p_T) = \tilde{f}(p_T)\left(\frac{N}{N-1}\right)^2 \exp\left[-\frac{1}{2(N-1)} \times \left(\frac{2p_T^2}{\langle p_T^2\rangle} + \frac{\overline{p_z^2}}{\langle p_z^2\rangle} + \frac{\overline{E^2}}{\langle E^2\rangle - \langle E\rangle^2} - \frac{2\overline{E}\langle E\rangle}{\langle E^2\rangle - \langle E\rangle^2} + \frac{\langle E\rangle^2}{\langle E^2\rangle - \langle E\rangle^2}\right)\right]. \tag{5}$$

The notation $\overline{X}$ indicates the average of X over the rapidity interval used; see Appendix A for details. These averages depend, of course, on p_T and should not be confused with global averages $\langle X\rangle$ [Eq. (3)] which characterize the parent distribution.

We would also like to emphasize that since Eq. (5) depends on the energy of the particle (not just momentum), it becomes clear that the EMCIC effects are larger on heavier particles at the same p_T. Thus we should expect that the proton spectra will be more suppressed than pion spectra. In what follows, we find that ignoring the $\overline{p_z^2}/\langle p_z^2\rangle$ term does not affect our results, since the numerator is small for the narrow rapidity windows used here, and the denominator is large. In discussions below, we set this term to zero.

B. Straw-man postulate of a universal parent distribution

Equations (1)–(5) are reminiscent of Fermi's "Golden Rule" [32,33], in which the probability for making a particular observation is given by the product of the squared matrix element and a quantity determined by available phase space. The first term represented the underlying physical process. In his original statistical model [32], Fermi originally assumed it to be a constant representing the volume in which emitted particles were produced; this is equivalent to setting $\tilde{f}(p)$ constant in Eq. (1). While surprisingly successful in predicting cross sections and pion spectra [34,35], the emission volume required to describe the data was considered unrealistically large [36]. Using the mean value theorem, Hagedorn [33] generalized the theory so that the "physics term" is the interaction matrix element, suitably averaged over all final states.

We wish to make no assumptions about the underlying physics (represented by $\tilde{f}$) driving the observed spectrum $\tilde{f}_c$. Rather, we wish to quantify the effect of changing the multiplicity N, which appears in the phase-space term.

In particular, in the following section, we compare measured single-particle spectra for different event classes.

We postulate that the parent distributions for, say, classes 1 and 2, are the same ($\tilde{f}_1 = \tilde{f}_2$). By Eq. (3), this implies $\langle p_\mu\rangle_1 = \langle p_\mu\rangle_2 \equiv \langle p_\mu\rangle$. In this case, the *only* reason that the observed spectra differ ($\tilde{f}_{c,1} \neq \tilde{f}_{c,2}$) is the difference in "multiplicity" $N_1 \neq N_2$; see Sec. II C for a discussion of N_1.

To eliminate the (unknown) parent distribution itself, we will study the ratio of observed p_T distributions, which, by Eq. (5) becomes

$$\frac{\tilde{f}_{c,1}(p_T)}{\tilde{f}_{c,2}(p_T)} = K\left(\frac{(N_2-1)N_1}{(N_1-1)N_2}\right)^2 \exp\left[\left(\frac{1}{2(N_2-1)} - \frac{1}{2(N_1-1)}\right)\left(\frac{2p_T^2}{\langle p_T^2\rangle} + \frac{\overline{E^2}}{\langle E^2\rangle - \langle E\rangle^2} - \frac{2\overline{E}\langle E\rangle}{\langle E^2\rangle - \langle E\rangle^2} + \frac{\langle E\rangle^2}{\langle E^2\rangle - \langle E\rangle^2}\right)\right], \tag{6}$$

where the constant K is discussed at the end of Sec. II C. As mentioned at the end of Sec. II A, numerically unimportant terms in p_z have been dropped.

Naturally, our postulate cannot be expected to be entirely correct; one may reasonably expect the mix of physical processes in $p + p$ collisions to differ from those in Au + Au collisions. Nevertheless, it is interesting to find the degree to which the change in single-particle spectra may be attributed *only* to finite-multiplicity effects. We will find that the postulate works surprisingly well in some regions and fails in others. As we will discuss, both the success and failure raise interesting and surprising possibilities.

C. Testing the postulate: How to treat the parameters

By our postulate, the phase-space factor affecting a p_T distribution is driven by four quantities. Three of them, $\langle p_T^2\rangle$, $\langle E^2\rangle$, and $\langle E\rangle$, characterize the parent distribution, while N is the number of particles in the final state. In general, increasing any one parameter decreases the effect of phase-space restrictions on the observed distributions. But what should we expect these values to be? They should characterize the relevant system in which a limited quantity of energy and momentum is shared. They are not, however, directly measurable and should only approximately scale

with measured values for at least the five following reasons discussed here.

First, the energy and momentum are shared among measured and unmeasured (neutrals, neutrinos, etc.) particles alike so that N should roughly track the measured event multiplicity $N_{\rm meas}$, but need not be identical to it.

Second, emission of resonances smears the connection between N and $N_{\rm meas}$; e.g., the emission of an ω meson that later decays into "secondary" particles ($\omega \to \pi\pi\pi$) increments N by unity, rather than by three, as far as other particles are concerned. This latter consideration also affects the kinematic parameters $\langle p_T^2\rangle$, $\langle E^2\rangle$, and $\langle E\rangle$. While energy and momentum are, of course, conserved in resonance decay, the aforementioned quantities themselves are not. Thus, one need not expect perfect correspondence between the appropriate kinematic parameters in Eq. (6) and the measured ones.

Third, even restricting consideration to primary particles, it is unclear that all of them should be considered in the relevant ensemble of particles sharing some energy and momentum. In particular, for space-time extended systems in high-energy collisions, the momentum extent of characteristic physics processes (e.g., string breaking) and causality in an approximately boost-invariant scenario suggest that rapidity slices of roughly unit extent should be considered separate subsystems [26]. Of course, the total available energy in any event is shared among *all* such subsystems; i.e., the midrapidity subsystem in one event will not have exactly the same available energy as that in another event. However, such fluctuations are to be expected in any case—surely individual collisions will differ from one another to some extent. Thus, we repeat our interpretation of the four parameters N, $\langle p_T^2\rangle$, $\langle E^2\rangle$, and $\langle E\rangle$: they characterize the scale, in energy and momentum, of the limited available phase space to an N-particle subsystem.

Fourth, Eqs. (1)–(6) are appropriate for fixed N, while we will be comparing with measured spectra selected by measured charged-particle multiplicity. Thus, N would inevitably fluctuate within an event class, even if we could ignore the above considerations. Naturally, high-multiplicity events contribute to spectra more than low-multiplicity events. Similarly, the average multiplicity in two-particle correlations is even more shifted to higher multiplicities.

Fifth, as already mentioned in Sec. II A, the kinematic parameters $\langle p_T^2\rangle$, $\langle E^2\rangle$, and $\langle E\rangle$ correspond to the parent distribution, which will only correspond identically to the measured one in the limit of infinite multiplicity (i.e., no EMCIC distortions). See also the discussion in Appendix B.

For all of these reasons, we will treat N, $\langle p_T^2\rangle$, $\langle E^2\rangle$, and $\langle E\rangle$ as free parameters when testing our postulate against data. Our aim is not to actually measure these quantities by fitting the data with Eq. (6); this is good, since our fits to the data only very roughly constrain our four parameters, as discussed in the next section. Rather, our much less ambitious goal is to see whether "reasonable" values of these parameters can explain the multiplicity evolution of the spectra.

To get a feeling for these values, we look at $p + p$ collisions at $\sqrt{s_{NN}} = 200$ GeV, simulated by the PYTHIA event generator (v6.319) [37]. In the model, we can identify primary particles, thus avoiding some of the issues discussed above. However, the fact that PYTHIA conserves momentum means that we access $\langle p_\mu^n\rangle_c$ as defined by Eq. (4), not the parameters of the parent distribution. Nevertheless, a scale for our expectations may be set. Table I summarizes the result for primary particles satisfying a varying cut on pseudorapidity where all particle decays were switched off in PYTHIA simulations. The results from simulations in which resonance decays were included are presented in Table II. These two tables gives us rough estimates of ranges of the total multiplicity and kinematic variables that one may expect. The bulk component of single-particle spectra is often estimated with Maxwell-Boltzmann distributions, with inverse slope parameters in the range $T \sim 0.15$–0.35 GeV. Again, simply for rough guidance, we list Maxwell-Boltzmann expectations for our kinematic parameters in Table III, assuming pion-dominated system.

TABLE I. For a given selection on pseudorapidity $|\eta| < \eta_{\rm max}$, the number and kinematic variables for primary particles from a PYTHIA simulation of $p + p$ collisions at $\sqrt{s_{NN}} = 200$ GeV are given. Units are GeV/c or (GeV/c)^2, as appropriate. 100k events were used, and all decays were switched off in simulations.

$\eta_{\rm max}$	$\langle N\rangle$	$\langle p_T^2\rangle_c$	$\langle p_z^2\rangle_c$	$\langle E^2\rangle_c$	$\langle E\rangle_c$
1.0	7.5	0.58	0.41	1.45	0.98
2.0	13.4	0.59	2.81	3.89	1.57
3.0	17.9	0.59	12.95	14.01	2.65
4.0	21.5	0.59	82.45	83.55	5.13
5.0	23.4	0.59	262.88	265.03	8.29
∞	23.6	0.59	275.23	276.4	8.48

Finally, a word about normalization—the quantity K which appears in Eq. (6). Not only energy and momentum but also discrete quantum numbers such as the strangeness and baryon number are conserved event by event, affecting the overall yield of a given particle species. For example, the related phenomenon of "canonical suppression" affects the ratio of yields for strange versus nonstrange particles, as multiplicity varies [38,39]. Since we restrict our attention to energy and momentum conservation and the effect on kinematic quantities, we are interested in the *shape* of the spectra ratio, as a function of particle momentum, and include a factor K in our Eq. (6), which should be of order, but not necessarily identical to, unity. We do not discuss it further.

TABLE II. For a given selection on pseudorapidity $|\eta| < \eta_{\rm max}$, the number and kinematic variables for final state particles (particle index KS = 1 in PYTHIA) from a PYTHIA simulation of $p + p$ collisions at $\sqrt{s_{NN}} = 200$ GeV are given. 100k events were generated, and default PYTHIA parameters were used in simulations. Units are GeV/c or (GeV/c)^2, as appropriate.

$\eta_{\rm max}$	$\langle N\rangle$	$\langle p_T^2\rangle_c$	$\langle p_z^2\rangle_c$	$\langle E^2\rangle_c$	$\langle E\rangle_c$
1.0	16	0.20	0.11	0.40	0.44
2.0	29	0.21	0.76	1.05	0.68
3.0	39	0.21	3.5	3.8	1.2
4.0	47	0.21	24	25	2.2
5.0	51	0.22	88	89	3.7

TABLE III. Average kinematic variables obtained from the Maxwell-Boltzmann distribution $f(p) = \frac{dN}{dp^3} \sim e^{-E/T}$ using nonrelativistic and ultrarelativistic limits. A pion gas is assumed.

	Nonrel. limit	Ultrarel. limit	If $T = 0.15$–0.35 GeV
$\langle p_T^2 \rangle$	$2mT$	$8T^2$	0.045–0.98 (GeV/c)^2
$\langle E^2 \rangle$	$\frac{15}{4}T^2 + m^2$	$12T^2$	0.10–1.50 GeV^2
$\langle E \rangle$	$\frac{3}{2}T + m$	$3T$	0.36–1.00 GeV

III. TEST OF THE POSTULATE: COMPARISON WITH DATA

We now explore the degree to which the postulate proposed above describes the multiplicity evolution of measured p_T spectra measured in $\sqrt{s_{NN}} = 200$ GeV collisions at RHIC. As is frequently done, we will separately discuss the soft ($p_T \lesssim 1$ GeV/c) and hard ($p_T \gtrsim 3$ GeV/c) portions of the spectra. This separation is not entirely arbitrary, as spectra in these two p_T ranges are thought to be dominated by quite different physics, and the multiplicity evolution in the two sectors is usually interpreted in terms of distinct physics messages.

In the soft sector, the spectral shapes are often consistent with hydrodynamic calculations, e.g., Refs. [18,40], or fitted with blast-wave type models, e.g., Refs. [19,41], and show evidence of strong, explosive flow associated with a collective bulk medium. This is especially clear in the mass dependence of the spectra; the m_T (or p_T) spectrum of heavy particles such as protons are significantly flatter than that for pions, in the presence of strong flow. The multiplicity evolution in this sector suggests that high-multiplicity collisions (say, central Au + Au collisions) show much more collective flow than do low-multiplicity (say, $p + p$) collisions [21]. Such an interpretation is initially sensible in a scenario in which flow is built up through multiple collisions among emitted particles; the concept of a collective bulk medium in a very low-multiplicity collision is thus usually considered questionable.

Particle yields at high p_T, on the other hand, are generally discussed in the context of fragments from high-Q^2 parton scatterings in the initial stage of the collision. As the event multiplicity in Au + Au collisions is increased, a suppression of high-p_T yields is observed, relative to a properly normalized minimum-bias spectrum from $p + p$ collisions. This suppression has been attributed to partonic energy loss in the bulk medium [42–45].

The multiplicity evolution of the spectra in $p + p$ collisions, however, shows quite the reverse. Relative to the soft sector, the high-p_T yields increase as the multiplicity increases; one may also say that the p_T spectra become less steep as multiplicity increases [23]. This seems to reinforce the conclusion discussed above in relation to the soft sector, that $p + p$ collisions do not build up a bulk system capable of quenching jets.

Here, we reconsider these conclusions based on the multiplicity evolution of the spectra, in light of the phase-space restrictions discussed above.

A. Soft sector: Identified particles in Au + Au versus $p + p$

Figure 1 shows m_T distributions for minimum-bias $p + p$ collisions and multiplicity-selected Au + Au collisions, all at

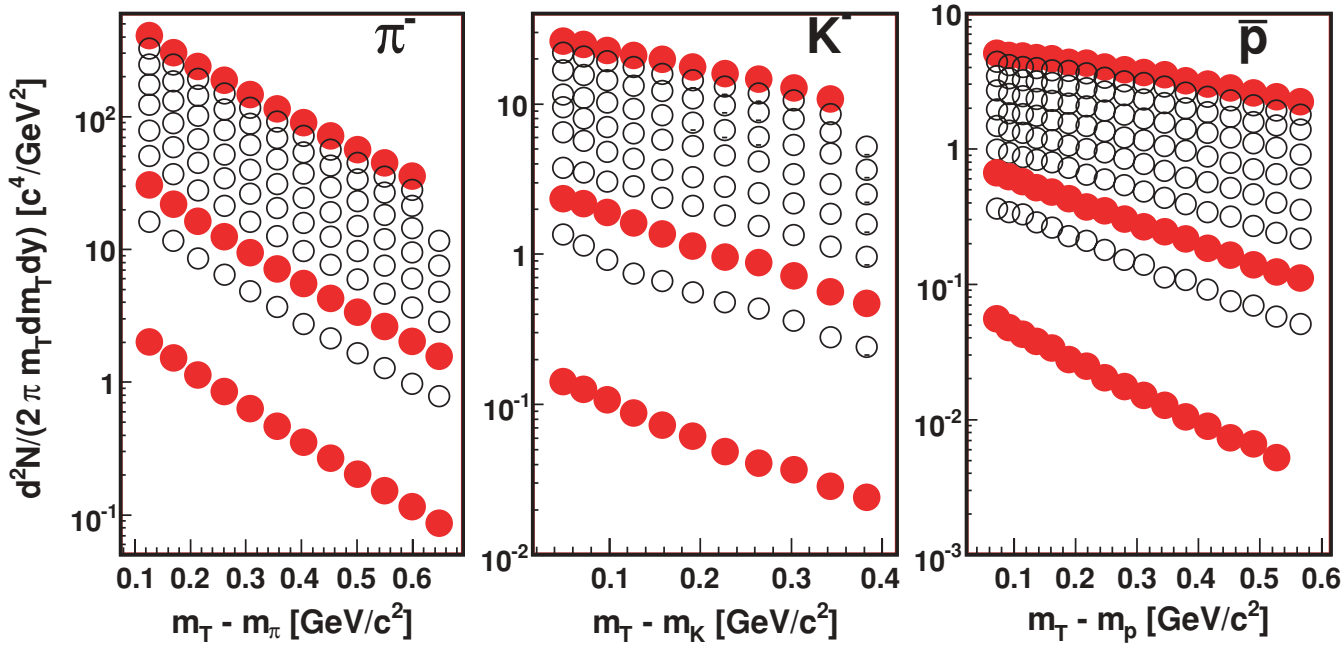

FIG. 1. (Color online) Transverse mass distributions for pions (left), kaons (center), and antiprotons (right) measured by the STAR Collaboration for $\sqrt{s_{NN}} = 200$ GeV collisions [21]. The lowest data points represent minimum-bias $p + p$ collisions, while the others come from Au + Au collisions of increasing multiplicity. Filled data points are for the top 5% and 60–70% highest multiplicity Au + Au collisions and for the $p + p$ collisions.

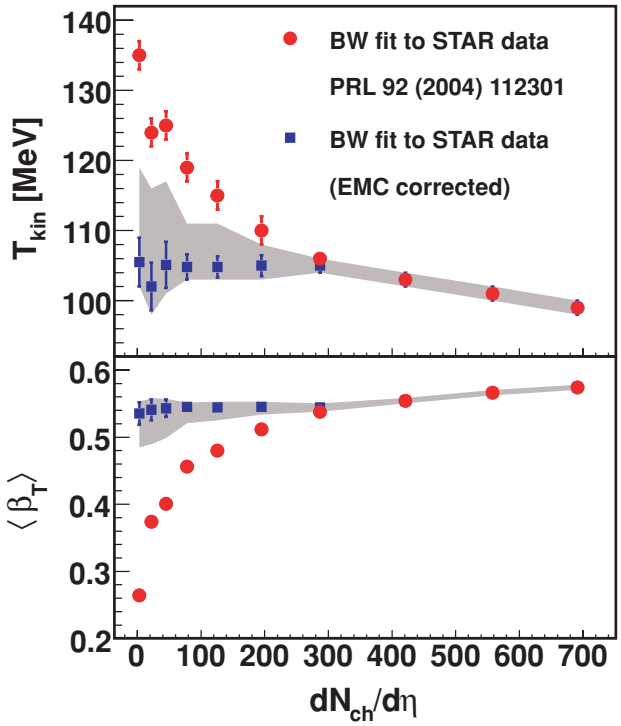

FIG. 2. (Color online) Temperature (top panel) and flow (bottom panel) parameters of a blast-wave model [19] fit to the STAR spectra of Fig. 1 (circles) and to EMCIC-corrected spectra (squares), as a function of the event multiplicity. The shaded region represents these results combined with systematic errors, as discussed in the text.

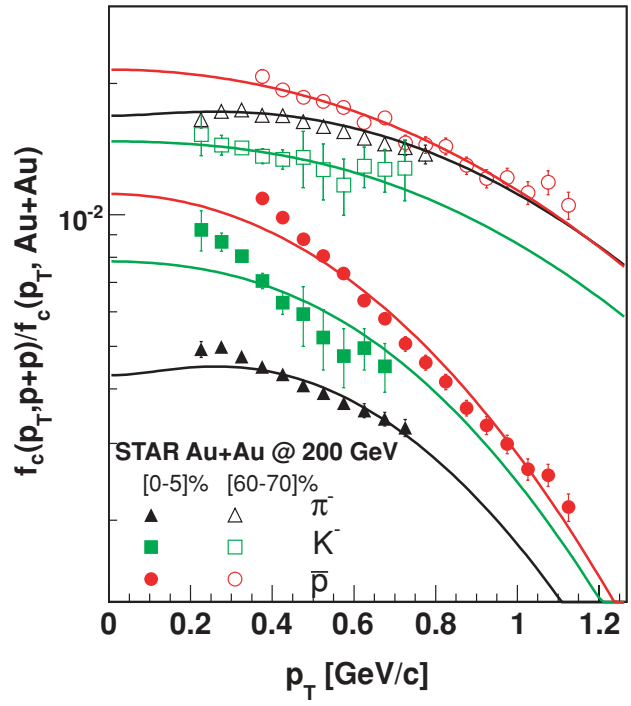

FIG. 3. (Color online) Ratio of the p_T distribution from minimum-bias $p + p$ collisions to the distribution from 0–5% (filled data points) and 60–70% (open data points) highest multiplicity Au + Au collisions; c.f. Fig. 1. The ratio of the kaon spectra from $p + p$ and 0–5% Au + Au collisions (solid squares) has been scaled by a factor 1.7 for clarity. Curves represent a calculation of this ratio (ratio of EMCIC factors) using Eq. (6).

$\sqrt{s_{NN}} = 200$ GeV, reported by the STAR Collaboration at RHIC [21]. For the highest multiplicity Au + Au collisions (top-most filled data points), the spectrum for heavier emitted particles is less steep than the essentially exponential pion spectrum. Circles in Fig. 2 show the result of fits with a blast-wave model [19]. They indicate a kinetic freeze-out temperature of about 100 MeV and average collective flow velocity about $0.6c$ for the most central collisions. For lower multiplicity collisions, the freeze-out temperature appears to grow to ∼130 MeV, and the flow velocity decreases to $\sim 0.25c$. The STAR Collaboration, using a slightly different implementation of a blast-wave model, reported essentially identical values [21].

Ratios of spectra from minimum-bias $p + p$ collisions to those from Au + Au collisions are plotted in Fig. 3. For the filled points, the denominator is the most central Au + Au collisions, while the open points represent the ratio when the denominator is from peripheral (60–70% centrality) Au + Au collisions. Pions, kaons, and protons are distinguished by different symbol shapes.

The curves show the function given in Eq. (6) for the kinematic scales given in Table IV. From the table it is clear that all curves in Fig. 3 are generated with the same kinematic variables $\langle p_T^2 \rangle$, $\langle E^2 \rangle$, and $\langle E \rangle$; only the relevant multiplicity changes.

We do not quote uncertainties on the kinematic or multiplicity parameters, as the fitting space is complex, with large correlations between them. Furthermore, it is clear that the calculated curves do not perfectly reproduce the measured ratios. However, it is also clear that "reasonable" values of multiplicity and energy-momentum scales go a long way toward explaining the multiplicity evolution of the spectra, even keeping physics (parent distribution) fixed. Our postulate of Sec. II B seems to contain a good deal of truth.

Another way to view the same results is useful. While the curves shown in Fig. 3 only approximately describe the data shown there, one may approximately "correct" the measured m_T distributions to account for EMCICs. This is shown in Fig. 4, where the measured mininum-bias $p + p$ and central and midperipheral Au + Au spectra have been copied from the full points of Fig. 1 and are shown as full points. The open red triangles represent the minimum-bias $p + p$ spectra, divided by Eq. (6), with the parameters from Table IV. This "EMCIC-corrected" spectrum is then scaled up to show comparison with the spectra from central Au + Au (open red circles); the level of (dis)agreement is identical to that between the lower data points and curves in Fig. 3.

Spectra from the mid-central Au + Au collisions have been likewise "corrected". The open squares in Fig. 4 may be compared with the open circles; again the level of (dis)agreement is equivalent to that between the upper data points and curves in Fig. 3.

Spectra themselves contain more information than two-parameter fits to spectra. However, much has been made of

TABLE IV. Multiplicity and parent-distribution kinematic parameters that give a reasonable description of the spectrum ratios for identified particles in the soft sector. See text for details. Note that the multiplicity changes with event class; the parent distribution is assumed identical.

Event selection	N	$\langle p_T^2 \rangle$ [(GeV/c)^2]	$\langle E^2 \rangle$ (GeV^2)	$\langle E \rangle$ (GeV)
$p + p$ min-bias	10.3	0.12	0.43	0.61
Au + Au 70–80%	15.2	”	”	”
Au + Au 60–70%	18.3	”	”	”
Au + Au 50–60%	27.3	”	”	”
Au + Au 40–50%	38.7	”	”	”
Au + Au 30–40%	67.6	”	”	”
Au + Au 20–30%	219	”	”	”
Au + Au 10–20%	>300	”	”	”
Au + Au 5–10%	>300	”	”	”
Au + Au 0–5%	>300	”	”	”

blast-wave fits to measured p_T spectra, which suggest a much larger flow in central Au + Au collisions, relative to $p + p$ collisions. Thus, it may be instructive to see how EMCICs affect these parameters. In Fig. 5, the p_T distributions for $p + p$ collisions and the six lowest multiplicity selections on Au + Au collisions are shown. Blast-wave fits to the measured spectra, resulting in the parameters shown by red triangles in Fig. 2 are shown as curves. On the linear scale of the figure, some deviation between the fit and data, particularly at the lowest p_T for the light particle, is seen. This has been observed previously in blast-wave fits and may be due to resonances [19,46]. Nevertheless, the fits to measured data are reasonable overall, and for simplicity, we do not exclude these bins.

Also shown in Fig. 5 are the EMCIC-corrected spectra, as discussed above. As already seen in Fig. 4, these differ from the measured spectra mostly for low-multiplicity collisions and for the heavier emitted particles. Blast-wave fits to these spectra are also shown. Especially for the very lowest multiplicity collisions, these fits are less satisfactory than those to the measured spectra; the parent distributions extracted via our approximate EMCIC

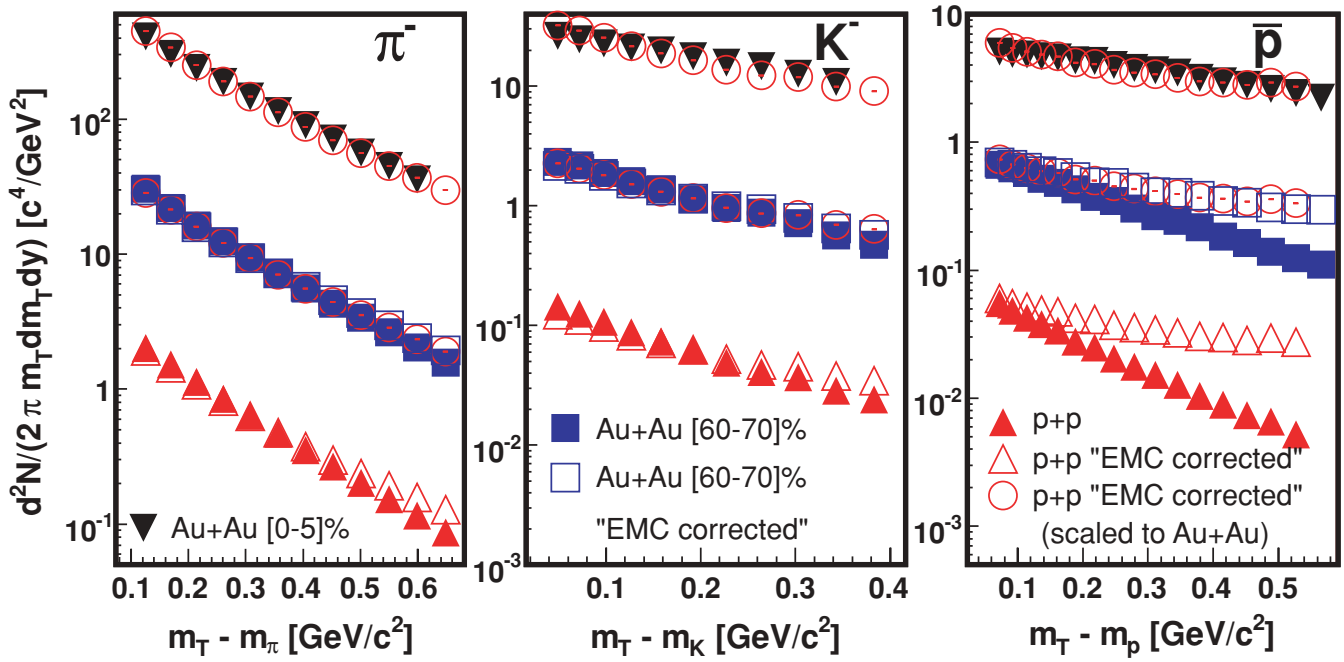

FIG. 4. (Color online) Transverse mass distributions of pions, kaons, and antiprotons for minimum-bias $p + p$ collisions and 60–70% and 0–5% highest multiplicity Au + Au collisions at $\sqrt{s_{NN}} = 200$ GeV. Filled data points are the same as in Fig. 1. Open triangles represent the $p + p$ spectra divided by the lower curves shown in Fig. 3. Open circles are the same spectra as the open triangles, except scaled up to compare with the spectra from the Au + Au collisions. Open squares represent the spectra from 60–70% highest multiplicity Au + Au events, divided by the ratio of upper and lower curves shown in Fig. 3. See text for details.

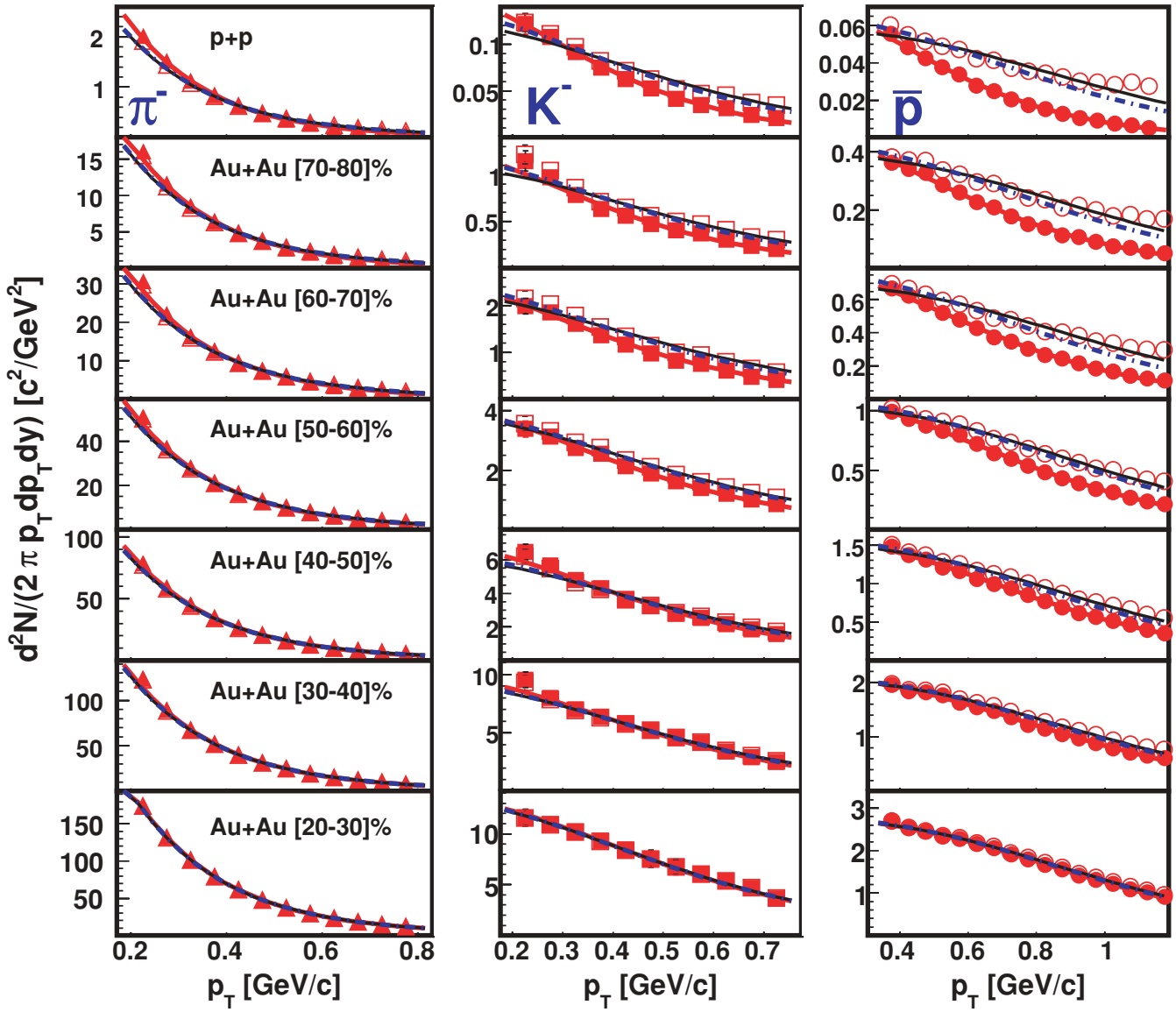

FIG. 5. (Color online) dN/dp_T^2 spectra for pions (left), kaons (center), and protons (right) are plotted on a linear scale, as a function of event multiplicity. Topmost panels show spectra for minimum-bias $p + p$ collisions, and the spectra for the six lowest multiplicity selections of Au + Au collisions are shown in the lower panels. Filled symbols are the measured data, while open symbols are the "EMCIC-corrected" distributions, discussed in the text. (For pions, these distributions overlap almost completely.) Blast-wave fits are indicated by the curves. For the EMCIC-corrected spectra, two fits are performed to estimate systematic errors: a fit to all data points (solid line) and a fit that ignores proton yields above $p_T = 0.8$ GeV/c (dashed line).

correction procedure follow the blast-wave shape only approximately. Much of the deviation is at $p_T \sim 0.9$ GeV/c for protons from the lowest multiplicity collisions (upper-right panels). This is the region around which the approximations used in deriving the EMCIC correction should start to break down, as discussed in Appendix B. So, two fits are performed: one including all data points shown (blue squares in Fig. 2), and the other excluding proton spectra points with $p_T > 0.8$ GeV/c. The resulting range of blast-wave parameters is indicated by the shaded region in Fig. 2. There, statistical errors on the fit parameters have been multiplied by $\sqrt{\chi^2/\text{d.o.f.}}$ (ranging from ∼2 for spectra from $p + p$ collisions to ∼1 for those from midperipheral and central Au + Au collisions) and added to both ends of the range. Thus, the shaded region should represent a conservative estimate of blast-wave temperature and flow strengths to the parent distributions.

In summary, to the extent that the curves in Fig. 3 describe the ratios shown there—which they do in sign, magnitude, and mass dependence but only approximately in shape—the data are consistent with a common parent distribution for spectra from all collisions. The residual deviation seen in Fig. 3 is observed again in different forms in Figs. 4 and 2. The upshot is that EMCICs may dominate the multiplicity evolution of the

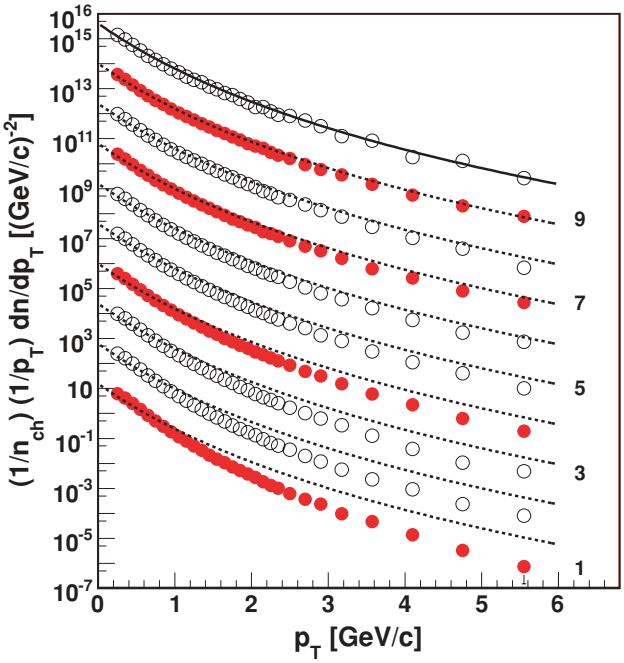

FIG. 6. (Color online) Transverse momentum spectra of unidentified negative hadrons from $p + p$ collisions at $\sqrt{s_{NN}} = 200$ GeV by the STAR Collaboration [23]. The lowest (highest) dataset corresponds to the lowest (highest) multiplicity collisions. The solid line is intended only to guide the eye and show the shape of the spectrum for the highest multiplicity selection. It is rescaled and redrawn as a dashed lines below to emphasize the multiplicity evolution of the spectrum shape.

spectra in the soft sector at RHIC. Extracting physics messages from the changing spectra, while ignoring kinematic effects of the same order as the observed changes themselves, seems unjustified.

In particular, the STAR Collaboration [21] and others [19] have fitted the spectra with blast-wave distributions, which ignore EMCIC effects. Based on these fits, they concluded that the difference in spectral shapes between high- and low-multiplicity collisions was due to much lower flow in the latter; c.f. Fig. 2. Recently, Tang *et al.* [47] arrived to the same conclusion, using a modified blast-wave fit based on Tsallis statistics. This requires introduction of an extra parameter q intended to account for system fluctuation effects [48]. However, contrary to the claims in the Tang paper, the Tsallis distribution, with or without q, does *not* account for energy and momentum conservation [49]; EMCIC effects would need to be added on top of the Tsallis statistics [49]. Therefore, conclusions about flow in low-multiplicity collisions based on these fits are suspect.

An independent measurement of flow would help clarify this issue. Two-particle femtoscopy (HBT) is a sensitive probe of collective motion [50] and has been measured in $p + p$ collisions at RHIC [51]. Any scenario should be able to describe simultaneously both the spectral shapes and the m_T dependence of the femtoscopic scales. A study of this topic is underway.

B. Soft sector: Unidentified particles in multiplicity-selected $p + p$ collisions

While minimum-bias $p + p$ collisions are the natural "reference" when studying Au + Au collisions, the STAR experiment has also measured p_T spectra from multiplicity-selected $p + p$ collisions [23]. These are reproduced in Fig. 6, in which the lowest multiplicity collisions are shown on the bottom and the highest at the top. Numerical labels to the right of the spectra are included just for ease of reference here.

The solid curve is a power-law fit to the highest multiplicity spectrum (#10), just for reference. This curve is scaled and replotted as dashed lines to make clear the multiplicity evolution of the spectra. Concentrating on the soft sector for the moment, we perform the same exercise as above, to see to what extent this multiplicity evolution can be attributed to EMCICs.

In Fig. 7 are shown three ratios of spectra, in which the second-highest multiplicity spectrum (#9) is used as the denominator, to avoid statistical fluctuations associated with the highest multiplicity spectrum. Also shown are curves, using Eq. (6) with the energy-momentum scales given in Table V.

The spectra reported by STAR are for unidentified negative hadrons. In calculating these curves, we assumed that all particles were pions. This matters, since the energy terms in Eq. (6) require the particle mass. We expect the energy-momentum scales listed in Table V to be affected by this simplistic assumption. To do better, particle-identified spectra from multiplicity-selected $p + p$ collisions would be required. Given this and the only semiquantitative agreement between the calculations and measured ratios shown in Fig. 7, we conclude only that the EMCIC contribution to the multiplicity evolution of low-p_T spectra in $p + p$ collisions is at least of the same order as the observed effect itself.

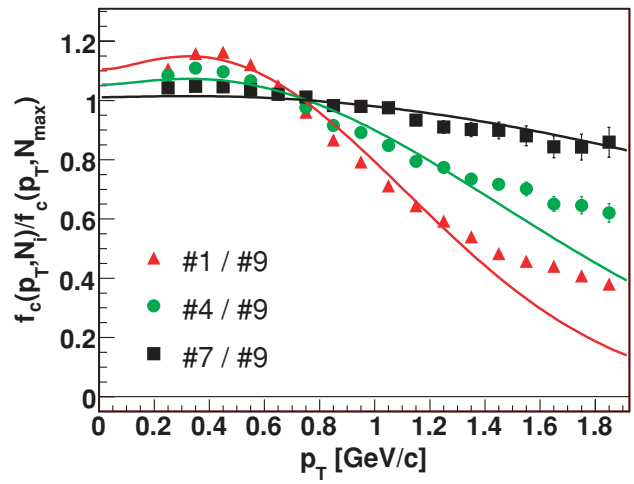

FIG. 7. (Color online) Ratio of the p_T spectra shown by full points in Fig. 6. Spectra for the lowest multiplicity (triangles), fifth-lowest (circles), and seventh-lowest (squares) multiplicity collisions are divided by the spectrum for the second-highest multiplicity collisions. Curves represent a calculation of this ratio (ratio of EMCIC factors) using Eq. (6); see text for details.

TABLE V. Multiplicity and parent-distribution kinematic parameters that give a reasonable description of the spectrum ratios for unidentified particles in the soft sector from multiplicity-selected $p+p$ collisions. See text for details. Note that the multiplicity changes with event class; the parent distribution is assumed identical.

Multiplicity cut	N	$\langle p_T^2\rangle$ [(GeV/c)^2]	$\langle E^2\rangle$ (GeV^2)	$\langle E\rangle$ (GeV)
# 1	6.7	0.31	0.90	0.84
# 4	11.1	”	”	”
# 7	24.2	”	”	”
# 9	35.1	”	”	”

C. Segue: From the soft to the hard sector

Figure 3 shows the central result of this paper, namely, that the multiplicity evolution of the mass and p_T dependence of single-particle spectra in the soft sector may be understood almost entirely in terms of phase-space restriction with decreasing event multiplicity.

Plotted in that figure is the ratio of spectra from low-multiplicity events over spectra from high-multiplicity events. Experimental studies sometimes show this ratio's inverse, often called R_{AA} [3]. While of course the same information is shown in both representations, we chose that of Fig. 3 for two reasons. The first is to emphasize the effects of EMCICs, the topic of this paper; these are, generically, to suppress the particle yield at high energy and momentum, particularly for low-N final states. (In multiparticle distributions, they also generate measurable correlations [25].)

The second reason is to stress that we have been discussing spectra in the soft sector, whereas the ratio R_{AA} is generally studied at high p_T. At large p_T, we expect that a purely EMCIC-based explanation of the multiplicity evolution of the spectra might break down, for two reasons. First, even if particles of all momenta shared phase space statistically, our approximation of Eq. (2) is expected to break down for energies much above the average energy, as discussed in Appendix B. Second, it is believed that the high-p_T yield has a large preequilibrium component; thus, high-p_T particles might participate less in the statistical sharing of phase space, as discussed in Sec. II C.

As we discuss in the next section, EMCICs surely do *not* dominate the multiplicity evolution of the hard sector in heavy ion collisions. For interpreting high-p_T spectra from multiplicity-selected $p+p$ collisions, accounting for EMCICs may or may not be important. To make the connection to Fig. 3, we will plot spectra from low-multiplicity collisions over those from high-multiplicity, as well as the inverse, to make the connection to R_{AA}.

D. Spectra in the hard sector

The generic effect of EMCICs is to suppress particle yields at energy and momentum far from their average values. The effect is stronger for lower multiplicity N. It is clear, then, that EMCICs cannot account for the multiplicity evolution of the spectra at high p_T in Au + Au collisions, since high-multiplicity collisions are observed to have *more* suppression at high p_T than do low-multiplicity collisions [3]. Thus, we conclude that our postulate fails for Au + Au collisions at high p_T; the parent distribution describing the underlying physics in this region does, indeed, change with multiplicity.

But in $p+p$ collisions, the multiplicity evolution in the hard sector is opposite to that in Au + Au collisions. In particular, in $p+p$ collisions, the yield at high p_T (relative to lower p_T) is *increased* as multiplicity increases, as is clear from Fig. 6; similar results have been observed in $\overline{p}+p$ collisions at Fermilab's Tevatron [52] and CERN's Intersecting Storage Rings (ISR) [53] and Sp$\overline{\text{p}}$S [54]. A "hardening" of the spectrum with increasing multiplicity goes in the same direction as would EMCIC effects. To what extent can EMCICs account for the multiplicity evolution of spectra from $p+p$ collisions in the hard sector?

Some insight into this question may be gained from Fig. 8, in which the data and curves shown in Fig. 7 are plotted out to $p_T = 6$ GeV/c. Clearly, the calculated suppression function [Eq. (6)] fails dramatically at high p_T.

We recall that Eqs. (2) and (6) are based on the central limit theorem (CLT), which naturally leads to Gaussian distributions. As discussed in Appendix B, one expects the breakdown of the CLT approximation in the far tails of the distribution, e.g., when $p_T^2 \gg \langle p_T^2\rangle$. Thus, any inferences we make about EMCIC effects in the hard sector remain qualitative. Nevertheless, the level of disagreement between the calculations and measurements leads us to conclude that EMCICs do *not* fully explain the multiplicity evolution of p_T spectra in $p+p$ collisions in the hard sector.

However, this in itself raises a fascinating possibility. Figure 8 shows that relative to high-multiplicity $p+p$ collisions, the suppression of high-p_T yields from low-multiplicity collisions is not as strong as one expects from our simple postulate. Said another way, the high-p_T "enhancement" in high-multiplicity collisions may not be as large as one expects from phase-space considerations alone. This is emphasized in

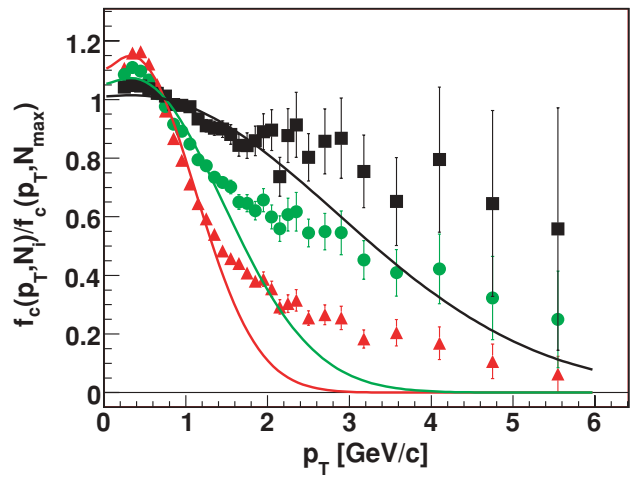

FIG. 8. (Color online) Same as Fig. 7, but plotted over the entire measured p_T range.

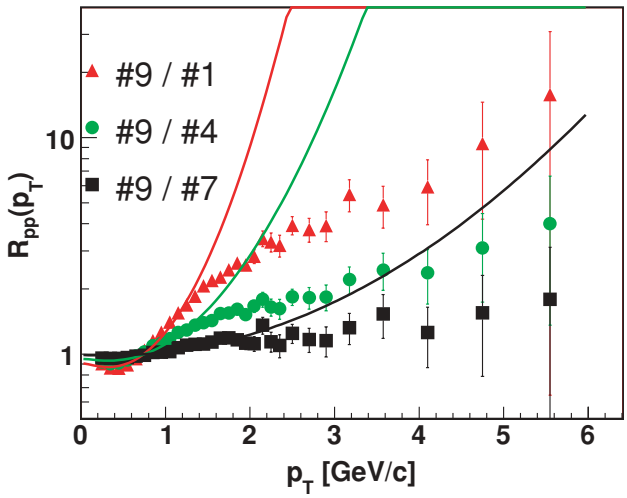

FIG. 9. (Color online) R_{pp}, the analog of R_{CP} used in heavy ion collisions. The spectrum from the highest multiplicity $p+p$ collisions are divided by spectra from lower multiplicity collisions (see filled data points in Fig. 6). The data and curves are simply the inverse of those shown in Fig. 8.

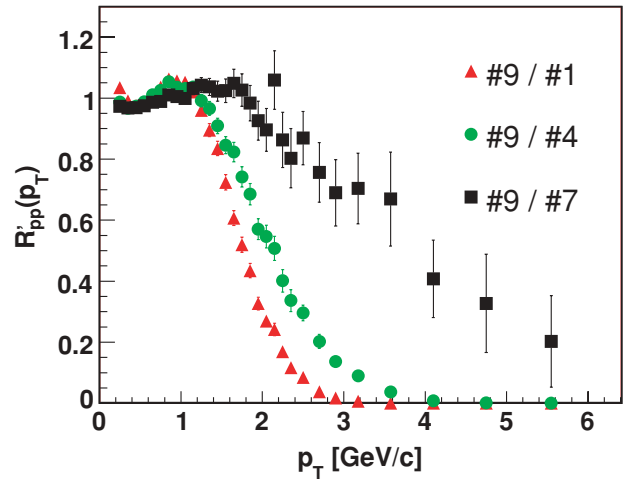

FIG. 10. (Color online) R_{pp} (c.f. Fig. 9) divided by the EMCIC contribution to R_{pp}, as calculated by Eq. (7).

Fig. 9, in which is plotted R_{pp}, the ratio of the spectrum from high-multiplicity to lower-multiplicity collisions; R_{pp} is the analog of R_{CP} from heavy ion collisions [3].

The motivation for studying quantities like R_{AA} and R_{CP} (and now R_{pp}) is to identify important differences between one class of collisions and another. Presumably, one is interested in physics effects (jet quenching, etc.), above and beyond "trivial" energy and momentum conservation. Thus, it makes sense to attempt to correct for EMCICs by dividing them out as we did in Sec. III A, keeping in mind the caveats just discussed.

The result of this exercise is shown in Fig. 10, in which the data points from Fig. 9 are divided by the curves from the same figure, to form a new quantity R'_{pp}. Explicitly, the circles in Fig. 10, which compare multiplicity selections #9 and #4, are given by

$$R'^{(\#9,\#4)}_{pp}(p_T) \equiv \frac{\frac{dn}{dp_T}\big|_{\#9}}{\frac{dn}{dp_T}\big|_{\#4}} \exp\left[\left(\frac{1}{2\,(N_{\#9}-1)} - \frac{1}{2\,(N_{\#4}-1)}\right) \times \left(\frac{2p_T^2}{\langle p_T^2\rangle} + \frac{(E-\langle E\rangle)^2}{\langle E^2\rangle - \langle E\rangle^2}\right)\right], \quad (7)$$

where the relevant quantities from Table V are used. Again, all particles are assumed to have pion mass. Qualitative though it is, Fig. 10 raises the possibility that when "trivial" EMCICs are accounted for, the high-p_T yield from high-multiplicity $p+p$ collisions is *suppressed* relative to low-multiplicity collisions, a trend in the same direction as that observed in Au + Au collisions.

In the hard sector, our estimates are mathematically and conceptually too simplistic to decide whether this implies jet quenching in high-multiplicity $p+p$ collisions. However, it is quite clear that conservation-induced phase-space restrictions might be sufficiently large in the hard sector, so that a high-p_T "enhancement" in high-multiplicity $p+p$ collisions turns into a "suppression" when these effects are accounted for. Extracting physics messages (e.g., about minijet production or jet quenching) from the multiplicity evolution of $p+p$ spectra is a nontrivial task, in light of this potentially huge background effect. At the very least, EMCICs should not be ignored, as they usually are, when extracting physics messages.

IV. SUMMARY AND DISCUSSION

The study of relativistic heavy ion collisions is, by its very nature, heavily dependent on comparative systematics. Physical models or hypotheses are most stringently tested when predictions for a given observable are compared with measurements for a range of global collision conditions. Even aside from specific models, much qualitative information may be gleaned simply through study of the evolution of an observable as collision conditions—quantified by global variables—change.

Since the goal is to probe an interaction or transition characterized by a dimensionful scale (confinement length ~1 fm), perhaps the most important global variable is event multiplicity, which on average reflects the size of the system generated in the collision.

Directly measurable is the multiplicity evolution of experimental observables. This evolution is driven by (1) the evolution of the underlying physics, which is of direct interest, and (2) kinematic phase-space restrictions (EMCICs), which are presumably less interesting. It may be hazardous to ignore the latter effect and make inferences on the former, particularly since phase-space restrictions have an obvious explicit multiplicity dependence. In this study, we have quantitatively estimated the degree to which phase-space restrictions may affect physics inferences based on measured data.

We have focused on the multiplicity evolution of single-particle spectra. In previous published studies, analyses that have ignored EMCICs have inferred much from this evolution. In particular, there have been conclusions that spectra from central Au + Au collisions exhibit greater collective radial flow than do those from peripheral Au + Au or $p+p$ collisions. Using an expression to approximately account for

EMCIC effects, we have shown that the multiplicity evolution of the spectra may be dominated by such effects, rather than any change in the underlying physics.

In particular, we have tested the extreme postulate that the driving physics, characterized by a parent distribution, is *identical* for $p + p$ collisions and Au + Au collisions of all centralities. Since the parameters characterizing the parent distribution and the system multiplicity N were fitted, our test is not perfect. Some multiplicity evolution of the parent distribution itself may exist and may not be easily separable from EMCICs. Our point is that, with "reasonable" parameters, much of the data systematics is readily understood in terms of a universal parent distribution in the soft sector, and similar high-p_T yield suppression in $p + p$ and Au + Au collisions.

In the soft sector ($p_T \lesssim 1$ GeV/c), this postulate worked surprisingly well. The changes in m_T distributions, as the collision multiplicity is changed, are almost entirely due to EMCICs. "Correcting" the spectra for EMCICs, an approximate procedure along the lines of Fermi's Golden Rule, reveals almost universal parent distributions.

While the spectra themselves carry more information than fits to the spectra, it was interesting to find that blast-wave fits to the EMCIC-corrected spectra show that low-multiplicity Au + Au collisions, and even $p + p$ collisions, are characterized by very similar flow and temperature values as for spectra from Au + Au collisions. This contrasts strongly with previous conclusions and assumptions about collectivity in small systems. Blast-wave [19,21] or modified Blast-wave [47] fits which ignore EMCICs may yield unreliable results for low-multiplicity final states.

The same analysis of p_T spectra of unidentified hadrons from multiplicity-selected $p + p$ collisions yielded similar results, though the multiplicity evolution of the spectra was only roughly explained by our postulate. This is to be expected, for several reasons. First, our approximate expression to account for EMCICs was based on the central limit theorem, which begins to break down for the very small multiplicities involved. Second, the lack of particle identification led to a simple assumption that all particles were pions. Nevertheless, it was clear that EMCICs can go a long way toward explaining the multiplicity evolution of the p_T spectra in the soft sector.

EMCIC effects on momentum distributions are expected to be large at higher p_T, where a single particle may consume much of the total available energy. However, the approximations behind our EMCIC factor should begin to break down at high p_T. Unlike our results in the soft sector, we would be on shaky ground to draw firm conclusions from our studies in the hard sector. Nevertheless, we applied our formalism to obtain a rough estimate of the magnitude of restricted phase-space effects at high p_T.

First, we immediately realized that the well-known high-p_T suppression for central Au + Au collisions cannot be explained by EMCICs, as these effects would cause the opposite behavior (i.e., high-p_T enhancement) from what is experimentally observed. Thus, our postulate fully breaks down at high p_T—there is a difference in the *physics* (parent distribution) in the hard sector.

Turning to the multiplicity evolution of p_T spectra from $p + p$ collisions, however, the measured effect goes in the same direction as that expected from EMCIC effects. Still keeping in mind the caveats behind our expression at high momentum, we estimated that the high-p_T enhancement expected from EMCICs should be at least as large as that observed in the data. Again, we do not conclude but *suggest* that the multiplicity evolution of the parent distributions in $p + p$ collisions might in fact reveal a high-p_T suppression for high-multiplicity collisions, reminiscent of the effect measured in heavy ion collisions.

V. CONCLUSIONS AND OUTLOOK

Our results suggest that the multiplicity evolution of the soft portion of the p_T spectra in collisions at RHIC is dominated by phase-space restrictions. Effects due to actual changes in physics (the parent distribution) are subdominant. This suggests one of two possibilities.

First, one may take the common assumption that the physics underlying the soft particles from $A + A$ and $p + p$ collisions is quite different, say, bulk behavior versus string breaking, respectively. In this case, our results suggest that single-particle spectra are too insensitive to distinguish very different physics scenarios, and physics conclusions (say, radial flow in $A + A$ collisions) based on them are questionable.

On the other hand, the single-particle spectra may well reflect the underlying physics. If energy and momentum conservation effects are taken into account, the low-p_T spectra indicate that $p + p$ collisions display as much collective radial flow as do Au + Au collisions. In the larger system, this collective behavior is usually considered to arise from a (perhaps only partially) thermalized *bulk* system.

The question naturally arises: isn't it impossible for a system as small as that created in a $p + p$ collision to form even a partially thermalized bulk system which develops flow? The answer is not obvious. After all, estimates set the timescale for *complete* thermalization in central Au + Au collisions below 1 fm/c [18,40], via a mechanism that may be driven more by fluctuating color fields than by classical rescattering processes (see Ref. [55] and references therein). Perhaps the possibility that similar processes have sufficient time to thermalize a system on the scale of $\sim$1 fm should not be dismissed out of hand.

Indeed, in the literature one finds frequent suggestions [53,56–60], based on single-particle spectra, that high-energy particle collisions generate flowing bulk systems and perhaps even quark-gluon plasma; see also the recent review by Weiner [61]. By partially removing the obscuring effects of EMCICs, we have more directly compared proton collisions with heavy ion collisions (at the same energy and measured with the same detector), for which a flow-based interpretation is generally well accepted.

If a bulk system *is* created in $p + p$ collisions, might it quench jets as the medium does in Au + Au collisions? This was, after all, the original proposition of Bjorken [62]. The signature of such quenching would be a suppression of particle yields at high p_T in high-multiplicity collisions, relative to those at lower multiplicity. While our formalism is

insufficiently reliable at high p_T to draw firm quantitative conclusions, such a suppression may possibly be present, though obscured by EMCICs in measured spectra.

Increased focus on the relationship between large and small systems created in ultrarelativistic collisions is called for. Experimental programs at the CERN Large Hadron Collider will very soon open up important avenues in this study. In particular, the experiments will measure first $p + p$ collisions at record collision energies, with event multiplicities similar to Cu + Cu or semiperipheral Au + Au collisions at RHIC. Soft sector p_T distributions will likely be among the first observations reported. Later, with identical acceptance and techniques, the same experiments will then measure much larger systems created in Pb + Pb collisions. The direct comparison afforded by these data should help answer the question of whether a bulk system created in hadronic collisions is qualitatively different than that created in collisions between the heaviest ions, or merely a smaller version of it.

The nature of relativistic heavy ion studies depends upon comparison of small and large collision systems, each of which may be driven by distinct, nontrivial physics processes. In performing such comparisons, we must not neglect the "trivial" effect of energy and momentum conservation, and its explicit dependence on collision size.

ACKNOWLEDGMENTS

We thank Drs. Paweł Danielewicz, Sean Gavin, Ulrich Heinz, Peter Jacobs, Fred James, Declan Keane, Joern Knoll, Scott Pratt, Sergei Voloshin, Grzegorz Wilk, and Bill Zajc for important suggestions and insightful discussions, and Mr. Evan Askanazi for some numerical calculations. This work was supported by the U.S. National Science Foundation under Grant No. PHY-0653432.

APPENDIX A: EMCIC FACTORS FOR RAPIDITY- AND ANGLE-INTEGRATED p_T DISTRIBUTIONS

Equation (2) gives the EMCIC correction factor to the triple differential spectrum $\tilde{f}(p)$. Experimental measurements often report p_T distributions integrated over angle and a range of rapidity, i.e.,

$$\tilde{f}_c(p_T) \equiv \frac{1}{4\pi y_{\max}} \int_0^{2\pi} d\phi \int_{-y_{\max}}^{y_{\max}} dy\, \tilde{f}_c(p_x, p_y, p_z, E). \quad \text{(A1)}$$

In the absence of a triple-differential measurement, we consider azimuthally symmetric distributions, and $\langle p_x^2 \rangle = \langle p_y^2 \rangle = \langle p_T^2 \rangle/2$. At midrapidity at RHIC, it is reasonable also to assume a boost-invariant parent distribution. In this case, only part of the EMCIC factor remains in the rapidity integral:

$$\tilde{f}_c(p_T) = \tilde{f}(p_T) \left(\frac{N}{N-1}\right)^2 \exp\left[\frac{-p_T^2}{(N-1)\langle p_T^2\rangle}\right] \frac{1}{2y_{\max}} \times \int_{-y_{\max}}^{y_{\max}} dy \exp\left[\frac{-1}{2(N-1)}\left(\frac{p_z^2}{\langle p_z^2\rangle} + \frac{E^2}{\langle E^2\rangle - \langle E\rangle^2} - \frac{2E\langle E\rangle}{\langle E^2\rangle - \langle E\rangle^2} + \frac{\langle E\rangle^2}{\langle E^2\rangle - \langle E\rangle^2}\right)\right]. \quad \text{(A2)}$$

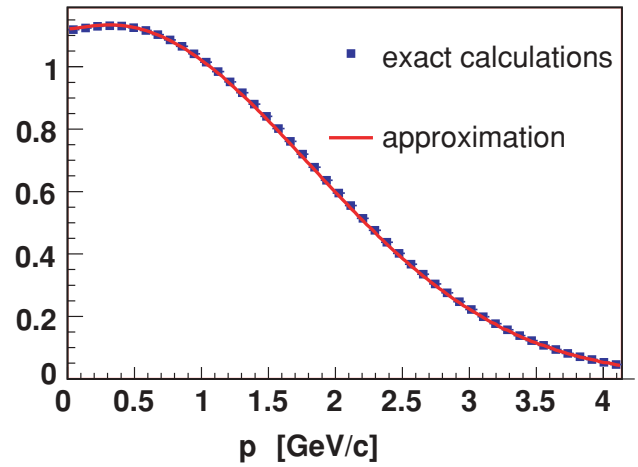

FIG. 11. (Color online) EMCIC factor calculated using the numerical averaging of Eq. (A2) and the approximation of Eq. (A3).

To arrive at a closed form for our EMCIC factor, we approximate the average of the exponential with the exponential of the average, i.e.,

$$\tilde{f}_c(p_T) = \tilde{f}(p_T) \left(\frac{N}{N-1}\right)^2 \times \exp\left[-\frac{1}{2(N-1)}\left(\frac{2p_T^2}{\langle p_T^2\rangle} + \frac{\overline{p_z^2}}{\langle p_z^2\rangle} + \frac{\overline{E^2}}{\langle E^2\rangle - \langle E\rangle^2} - \frac{2\overline{E}\langle E\rangle}{\langle E^2\rangle - \langle E\rangle^2} + \frac{\langle E\rangle^2}{\langle E^2\rangle - \langle E\rangle^2}\right)\right]. \quad \text{(A3)}$$

This expression is reproduced in Eq. (5).

Here, the rapidity-averaged quantities are

$$\overline{p_z^2} \equiv \frac{1}{2y_{\max}} \int_{-y_{\max}}^{y_{\max}} p_z^2\, dy = m_T^2 \left(\frac{\sinh(2y_{\max})}{4y_{\max}} - \frac{1}{2}\right), \quad \text{(A4)}$$

$$\overline{E^2} \equiv \frac{1}{2y_{\max}} \int_{-y_{\max}}^{y_{\max}} E^2 dy = m_T^2 \left(\frac{\sinh(2y_{\max})}{4y_{\max}} + \frac{1}{2}\right), \quad \text{(A5)}$$

$$\overline{E} \equiv \frac{1}{2y_{\max}} \int_{-y_{\max}}^{y_{\max}} E\, dy = m_T \frac{\sinh(y_{\max})}{y_{\max}}. \quad \text{(A6)}$$

The approximation used in going from Eq. (A2) to (A3) is well justified for typical numerical values used in this study. Figure 11 shows a numerical integration of the EMCIC factor from Eq. (A2) (labeled "exact") and Eq. (A3) ("approximation") for values indicated in the figure.

APPENDIX B: REGION OF APPLICABILITY FOR THE EMCIC FORMULA

The exact expression for the phase-space integral of Eq. (1) was approximated by that in Eq. (2) through an appeal to the central limit theorem. Discrepancies between the exact expression and the approximate Gaussian functional form will become more apparent in the tails of the distribution. For example, our approximate phase-space suppression function never vanishes, thus permitting a tiny but finite probability for a particle to carry more energy than that of the entire system!

In this appendix, we perform simple numerical calculations with the GENBOD computer program [63] to estimate the range of quantitative reliability of Eq. (2).

Given a total energy $E_{\rm tot}$, multiplicity N, and list of particle masses, GENBOD produces phase-space-weighted events of N four-momenta by filling Lorentz-invariant phase space according to the Fermi distribution,

$$\tilde{f} \equiv 2E\frac{d^3N}{dp^3} = \frac{1}{2\pi p}\frac{dN}{dE} \propto e^{-E/\zeta}, \tag{B1}$$

where ζ characterizes the slope of the energy distributions. Since it is $(1/p) \times dN/dE$ which is exponential and not $(1/(pE)) \times dN/dE$, the inverse slope ζ should not be considered a "temperature," but only a parameter characterizing the parent distribution.

As a result, generated particles in an event are correlated only by energy and momentum conservation. Thus, EMCIC effects on the calculated single-particle spectrum, $\tilde{f}_c(p)$, are given precisely according to Eq. (1).

To evaluate the region of validity of Eq. (2), we use Eq. (B1) as a parent distribution, $\tilde{f}(p)$. Results of this exercise are presented on Fig. 12, which shows energy spectra from GENBOD events with the same average energy per particle $\langle E\rangle_c = E_{\rm tot}/N = 1$ GeV, but different multiplicity N. As expected, in the limit of large N, $\tilde{f}_c(p) \to \tilde{f}(p)$, and it is clear that the plotted distribution is increasingly well described by an exponential, as N increases.

It is appropriate here to point out why we wish to identify the parent distribution in the first place, rather than following the procedure outlined in Sec. II B. There, the parent distribution cancels when taking the ratio of two measured spectra $\tilde{f}_{c,1}/\tilde{f}_{c,2}$, using the postulate that the parent distributions $\tilde{f}_1$ and $\tilde{f}_2$ are identical. In contrast, the parent distributions for the different GENBOD spectra shown in Fig. 12 are assuredly *not* the same. Those spectra came from event samples having the same $\langle E\rangle_c$ [c.f. Eq. (4)] and thus *different* $\langle E\rangle$ [c.f. Eq. (3)], implying different parents.

Having at hand a functional form for the GENBOD parent distribution, we may test our approximate formula for the phase-space modification factor by fitting the calculated

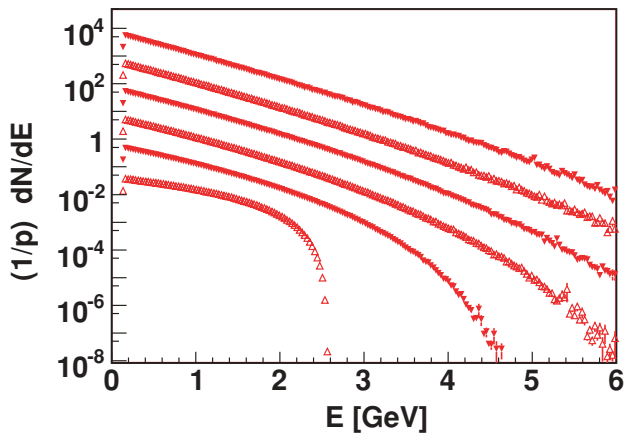

FIG. 12. (Color online) $\frac{1}{p}\frac{dN}{dE}$ obtained from GENBOD events run for the same average energy ($\langle E\rangle_c = 1$ GeV) but different multiplicities: $N = 5, 10, 15, 20, 30, 40$ pions.

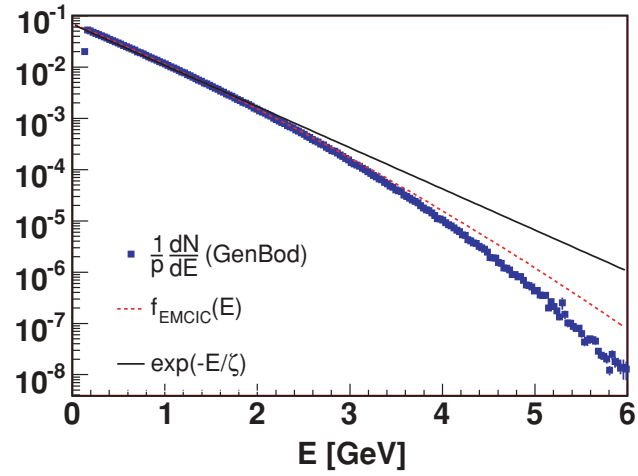

FIG. 13. (Color online) Blue points are $\frac{1}{p}\frac{dN}{dE}$ obtained from GENBOD events run for $N = 20$, $\langle E\rangle = 1$ GeV. Black solid curve is an exponential, the assumed parent distribution; c.f. Eq. (B1). Red dashed curve is the exponential times the EMCIC factor, as per Eq. (B2).

spectrum according to

$$\frac{dN_c}{dE} = Ape^{-E/\zeta}\left(\frac{N}{N-1}\right)^2 \exp\left[\left(-\frac{1}{2(N-1)}\right)\left(\frac{3p^2}{\langle p^2\rangle} + \frac{E^2}{\langle E^2\rangle - \langle E\rangle^2} - \frac{2E\langle E\rangle}{\langle E^2\rangle - \langle E\rangle^2} + \frac{\langle E\rangle^2}{\langle E^2\rangle - \langle E\rangle^2}\right)\right], \tag{B2}$$

where we used the fact that GENBOD generates particles isotropically so that $\langle p_x^2\rangle = \langle p_y^2\rangle = \langle p_z^2\rangle = \frac{1}{3}\langle p^2\rangle$. Since N is a known quantity, and $\langle E\rangle$, $\langle E^2\rangle$, and $\langle p^2\rangle$ may be directly calculated from ζ, the fit of Eq. (B2) has only two parameters:

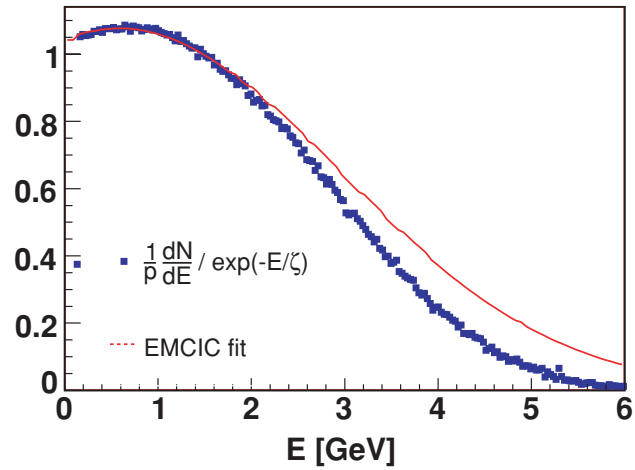

FIG. 14. (Color online) Blue points are $\frac{1}{p}\frac{dN}{dE}$ obtained from GENBOD events run for $N = 20$, $\langle E\rangle = 1$ GeV, divided by $\exp(-E/\zeta)$, i.e., the blue points from Fig. 13 divided by the black full curve from the same figure. Red dotted line is the EMCIC factor, i.e., the red dotted curve from Fig. 13 divided by the black full curve from the same figure.

the overall normalization A, which is unimportant to us, and ζ, which characterizes the parent distribution.

The results are shown in Fig. 13 and, for better detail, in Fig. 14. For the case here, which is typical of that in the data, we see that our approximation begins to break down for particle energies $E \gtrsim (2\text{–}3)\langle E\rangle$. Above this range, our approximation [e.g., Eq. (6)] should only be taken qualitatively.

[1] M. Gyulassy and M. Plumer, Phys. Lett. **B243**, 432 (1990).
[2] R. Baier, D. Schiff, and B. G. Zakharov, Annu. Rev. Nucl. Part. Sci. **50**, 37 (2000).
[3] K. Adcox *et al.* (PHENIX Collaboration), Phys. Rev. Lett. **88**, 022301 (2002).
[4] J. Adams *et al.* (STAR Collaboration), Phys. Rev. Lett. **91**, 072304 (2003).
[5] R. S. Bhalerao, J.-P. Blaizot, N. Borghini, and J.-Y. Ollitrault, Phys. Lett. **B627**, 49 (2005).
[6] M. Gyulassy and L. McLerran, Nucl. Phys. **A750**, 30 (2005).
[7] H. G. Ritter, in *CPOD2006 Proceedings*, PoS(CPOD2006)0159 (SISSA, Trieste, Italy, 2006).
[8] S. Nagamiya, Nucl. Phys. **A488**, 3c (1988).
[9] M. J. Tannenbaum, Rep. Prog. Phys. **69**, 2005 (2006).
[10] E. V. Shuryak, Phys. Rep. **61**, 71 (1980).
[11] E. V. Shuryak and I. Zahed, Phys. Rev. D **70**, 054507 (2004).
[12] F. Karsch, Lect. Notes Phys. **583**, 209 (2002).
[13] F. Becattini and U. W. Heinz, Z. Phys. C **76**, 269 (1997).
[14] P. Braun-Munzinger, J. Stachel, J. P. Wessels, and N. Xu, Phys. Lett. **B344**, 43 (1995).
[15] J. Letessier, A. Tounsi, U. W. Heinz, J. Sollfrank, and J. Rafelski, Phys. Rev. D **51**, 3408 (1995).
[16] P. Danielewicz *et al.*, Phys. Rev. C **38**, 120 (1988).
[17] N. Borghini, P. M. Dinh, and J.-Y. Ollitrault, Phys. Rev. C **62**, 034902 (2000).
[18] P. F. Kolb and U. W. Heinz, in *Quark-Gluon Plasma 3*, edited by R. C. Hwa and X.-N. Wang (World Scientific, Singapore, 2004).
[19] F. Retiere and M. A. Lisa, Phys. Rev. C **70**, 044907 (2004).
[20] R. J. Fries, B. Muller, C. Nonaka, and S. A. Bass, Phys. Rev. Lett. **90**, 202303 (2003).
[21] J. Adams *et al.* (STAR Collaboration), Phys. Rev. Lett. **92**, 112301 (2004).
[22] W. A. Zajc *et al.* (PHENIX Collaboration), Nucl. Phys. **A698**, 39 (2002).
[23] J. Adams *et al.* (STAR Collaboration), Phys. Rev. D **74**, 032006 (2006).
[24] M. C. Foster, D. Z. Freedman, S. Nussinov, J. Hanlon, and R. S. Panvini, Phys. Rev. D **6**, 3135 (1972).
[25] Z. Chajecki and M. Lisa, Phys. Rev. C **78**, 064903 (2008).
[26] N. Borghini, Phys. Rev. C **75**, 021904(R) (2007).
[27] N. Borghini, Eur. Phys. J. C **30**, 381 (2003).
[28] F. Becattini and L. Ferroni, Eur. Phys. J. C **52**, 597 (2007).
[29] H.-J. Drescher, J. Aichelin, and K. Werner, Phys. Rev. D **65**, 057501 (2002).
[30] K. Werner and J. Aichelin, Phys. Rev. C **52**, 1584 (1995).
[31] J. Knoll, Nucl. Phys. **A343**, 511 (1980).
[32] E. Fermi, Prog. Theor. Phys. **5**, 570 (1950).
[33] R. Hagedorn, Nuovo Cimento **15**, 434 (1960).
[34] W. Barkas *et al.* (Antiproton Collaboration Experiment), Phys. Rev. **105**, 1037 (1957).
[35] F. Cerulus, Nuovo Cimento **14**, 827 (1959).
[36] O. Chamberlain, G. Golbhaber, L. Janeau, T. Kalogeropoulos, E. Segrè, and R. Silberberg, Phys. Rev. **113**, 1615 (1959).
[37] T. Sjostrand *et al.*, Comput. Phys. Commun. **135**, 238 (2001).
[38] A. Tounsi and K. Redlich, arXiv:hep-ph/0111159.
[39] O. Fochler, S. Vogel, M. Bleicher, C. Greiner, P. Koch-Steinheimer, and Z. Xu, Phys. Rev. C **74**, 034902 (2006).
[40] P. Huovinen and P. V. Ruuskanen, Annu. Rev. Nucl. Part. Sci. **56**, 163 (2006).
[41] E. Schnedermann, J. Sollfrank, and U. W. Heinz, Phys. Rev. C **48**, 2462 (1993).
[42] J. Adams *et al.* (STAR Collaboration), Nucl. Phys. **A757**, 102 (2005).
[43] K. Adcox *et al.* (PHENIX Collaboration), Nucl. Phys. **A757**, 184 (2005).
[44] B. B. Back *et al.*, Nucl. Phys. **A757**, 28 (2005).
[45] I. Arsene *et al.* (BRAHMS Collaboration), Nucl. Phys. **A757**, 1 (2005).
[46] W. Broniowski and W. Florkowski, Phys. Rev. Lett. **87**, 272302 (2001).
[47] Z. Tang *et al.*, arXiv:0812.1609.
[48] G. Wilk and Z. Wlodarczyk, arXiv:0810.2939.
[49] G. Wilk (private communication).
[50] M. Lisa, S. Pratt, R. Soltz, and U. Wiedemann, Annu. Rev. Nucl. Part. Sci. **55**, 311 (2005).
[51] Z. Chajecki (STAR Collaboration), Nucl. Phys. **A774**, 599 (2006).
[52] T. Alexopoulos *et al.*, Phys. Rev. Lett. **60**, 1622 (1988).
[53] A. Breakstone *et al.* (Ames-Bologna-CERN-Dortmund-Heidelberg-Warsaw Collaboration), Z. Phys. C **33**, 333 (1987).
[54] G. Arnison *et al.* (UA1 Collaboration), Phys. Lett. **B118**, 167 (1982).
[55] S. Mrowczynski and M. H. Thoma, Annu. Rev. Nucl. Part. Sci. **57**, 61 (2007).
[56] L. Van Hove, Phys. Lett. **B118**, 138 (1982).
[57] P. Levai and B. Muller, Phys. Rev. Lett. **67**, 1519 (1991).
[58] T. Alexopoulos *et al.*, Phys. Lett. **B528**, 43 (2002).
[59] T. Alexopoulos *et al.*, Phys. Rev. Lett. **64**, 991 (1990).
[60] P. Steinberg, Nucl. Phys. **A752**, 423 (2005).
[61] R. M. Weiner, Int. J. Mod. Phys. E **15**, 37 (2006).
[62] J. D. Bjorken, FERMILAB-PUB-82-059-THY, 1982 (unpublished).
[63] F. James, CERN-68-15, 1968 (unpublished), available at http://doc.cern.ch/cernrep/1968/1968-015/1968-015.html.